

From Chills to Thrills: Revolutionizing Energy Efficiency and Load Flexibility in Supermarket Refrigeration

Ramin Faramarzi, National Renewable Energy Laboratory
Sammy Houssainy, National Renewable Energy Laboratory
Alexander Bulk, National Renewable Energy Laboratory

ABSTRACT

Open-vertical medium-temperature refrigerated display cases comprise nearly 50% of total case lineups in a typical supermarket, with more than 80% of their cooling load attributed to infiltration of warm and moist air from the surrounding space. The infiltration takes place across the air curtain system of the display case. While the air curtain acts as a thermal shield and as a cooling mechanism to maintain product temperature, it also entrains large amounts of heat and moisture from the adjacent space. Additionally, from food safety and quality standpoints, these fixtures are vulnerable to electric outages and traditionally cannot participate in load flexibility events.

This paper describes key features of an innovative design of a self-contained, water-cooled, medium-temperature, open-vertical display case. The novel concept will eliminate the inefficient air curtain system and incorporate a hybrid radiant and low-airflow convective cooling design with a thermal-energy-storage-coupled heat exchanger integrated into the refrigeration circuit. The focus of this paper is on evaluating the thermal performance of the novel hybrid design in maintaining target product temperature. It presents thermal performance findings from thermo-fluid system modeling and robust state-of-the-art laboratory experiments used to validate those models. Load flexibility attributes from thermal energy storage are not discussed.

A controlled-environment chamber at the National Renewable Energy Laboratory was leveraged to validate the thermal performance of the novel technology. Final results from bench-scale experiments indicate the proposed design maintained mean product temperatures within food safety guidelines.

Introduction

With roughly 68 kWh/sf-yr electric usage intensity (EUI), supermarkets have the second-highest EUI in the commercial buildings sector (EIA 2018). Refrigeration accounts for roughly 50% of the electric energy consumption in supermarkets. Open-vertical, medium-temperature refrigerated display cases (OVDC) comprise nearly 50% of total case lineups in a typical supermarket, with more than 80% of their total cooling load attributed to infiltration of air from the surrounding space (ASHRAE 2022).¹

OVDCs primarily use air to cool food products via convective heat transfer (Figure 1). A constant-volume fan system discharges a jet of cold air from a grille at the top-front edge of the case. The jet of air changes its thermal characteristics by entraining warm and moist air from the

¹ Prior research has shown that retrofitting this class of display cases with glass doors can yield significant energy efficiency improvements (Faramarzi, 2002). Nevertheless, the industry still considers glass doors in medium-temperature applications as an extra barrier between the shopper and merchandise, which can adversely impact sales. Therefore, the focus of this research is mainly on improving performance of open vertical fixtures.

sales area by the time it reaches the return air grille at the front-bottom edge of the case. Concurrently, due to the conservation of mass coupled with inefficient design of the air curtain system, a portion of refrigerated air spills out in front of the case. This cold spillage adversely affects shoppers' comfort. As the return air travels across the cold evaporator surface, the moisture content of air condenses and freezes on the coil. Frost formation on the coil surface acts as insulation and hampers heat transfer effectiveness between refrigerant and air. Additionally, it reduces the air passageway, resulting in cooling deprivation of food products. Therefore, these systems must undergo several defrost cycles per day. Defrost cycles adversely impact product temperature and case load. The heat of refrigeration of a baseline air-cooled, self-contained OVDC is typically rejected to the sales area. This waste heat increases the sales area's air conditioning load and cannot be reclaimed usefully for enhancing the capacity and/or efficiency of other building energy systems such as space or water heating.

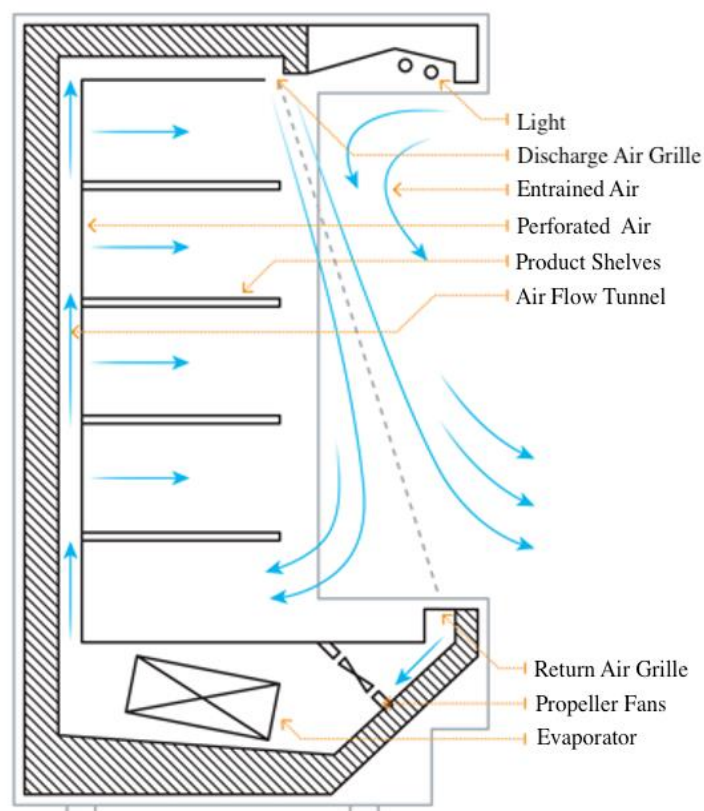


Figure 1. Current state of technology.

The baseline technology has the following key shortcomings, limitations, and challenges that will be addressed by the proposed hybrid system:

- High energy use due to large quantity of air infiltration that accounts for 80% of the cooling load
- Frost formation on the evaporator that restricts air flow and hampers heat transfer and further degrades energy efficiency due to the load required to remove the frost
- Highly variable and non-uniform product temperature distribution (up to 10°F) across the case product loading area

- Spilled cold air in the shopper aisles that adversely impacts human comfort
- Inability to participate in demand response events and load shaving/shifting strategies (Hirsch et al. 2015) (not addressed in this paper)
- For self-contained air-cooled units, the refrigeration heat rejected into the sales floor cannot be reclaimed usefully, resulting in increased air conditioning cooling load

Proposed Innovation

The proposed technology is based on a novel design approach that closely integrates the display case's refrigeration system with the heating, ventilating, and air conditioning (HVAC) and water heating systems, while enabling the case to serve as a flexible grid resource. This design incorporates energy efficiency and load flexibility by utilizing thermal energy storage (TES) and a hybrid cooling mechanism that relies on both radiant and low-airflow convective cooling (Figure 2). Although not discussed in this paper, the TES component of this novel design will utilize advanced phase change material.

The following figures depict schematic diagrams of the hybrid system, which eliminates the traditional air curtain design, and combines radiant and forced convection cooling mechanisms. A down-sized water-cooled vapor compression system, using propane (R-290) as refrigerant, charges the TES system which acts as an evaporator (lower diagram). A glycol loop discharges the TES by circulating chilled glycol into radiant panels and a small air/glycol heat exchanger (Figure 3). A fan circulates the warm return air through a small cooling coil and delivers low-volumetric flow rates through the perforated back panel to enhance product temperature maintenance.

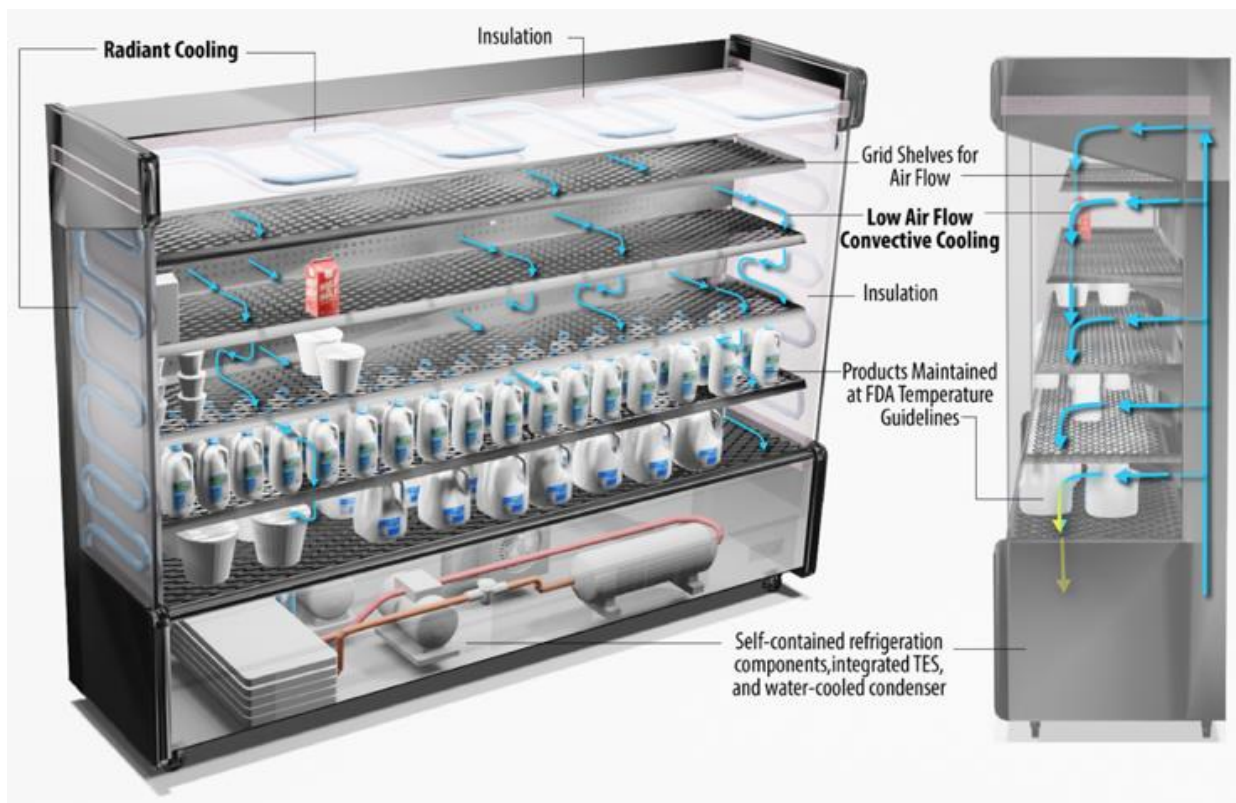


Figure 2. Proposed hybrid-cooled OVDC with an integrated TES.

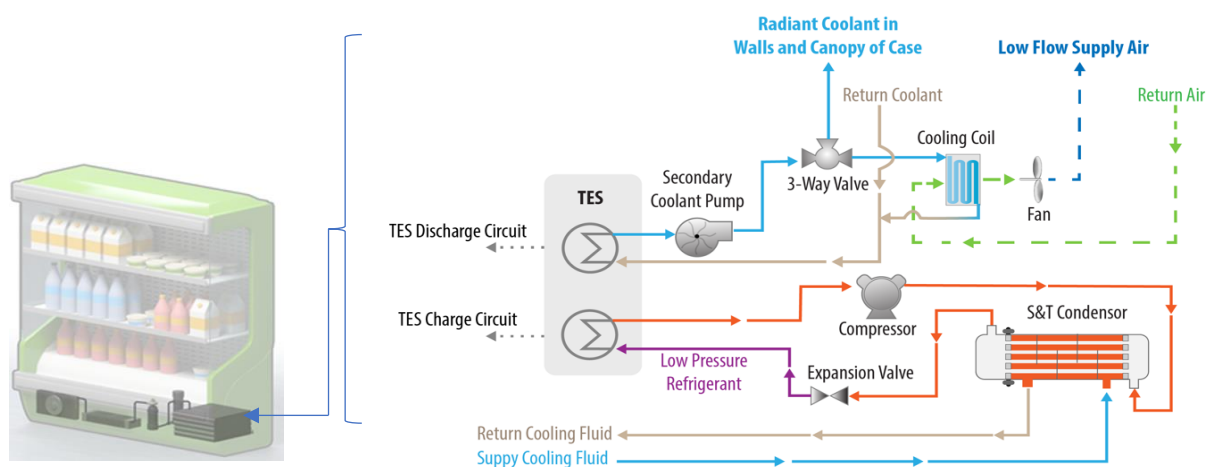


Figure 3. Approximate location of the proposed hybrid display case with an integrated, TES-coupled heat exchanger, and the proposed refrigeration cycle diagrams showing the TES charge circuit and TES discharge circuit.

The key benefits of the hybrid cooling technology and the specific design characteristics that achieve the desired outcome are:

- **Energy Efficiency:** (1) Reduces infiltration cooling load, frost, defrost cycles, and post-defrost pull-down loads through a design that eliminates the air curtain and includes radiant cooling; (2) Integrates with building space heating and water heating systems, which enables 100% waste heat recovery when needed and reduces overall building energy consumption; (3) Reduces condensing saturation temperature by rejecting heat to a water loop instead of air.
- **Demand Flexibility:** The design allows each case to operate independently and provides greater peak shaving and load dispatchability under critical peak demand periods by leveraging the TES and advanced controls in response to grid signals.
- **Affordability:** Energy savings associated with eliminating the air curtain infiltration and inefficient defrost cycles and peak demand reductions are expected to reduce operational costs and outweigh the incremental investments in the novel design. With supermarket demand costs that are potentially higher than consumption costs during on-peak periods, demand reduction in particular is expected to expand large monthly cost savings, thereby enhancing tight profit margins for owners (Jackson 2020).
- **Occupant Comfort:** Improved customer comfort is expected through a reduction in the otherwise substantial cold air spillage in shopping aisles.

Approach

The project approach includes extensive modeling, laboratory experiments, design of the hybrid cooling mechanism and TES system, integration of energy efficiency and load flexibility systems, and controls for grid interactivity. Figure 4 shows the integrated research approach to achieve the project goal. The following summarizes the key stages of this project:

1. Extensive literature search
2. Development of a robust thermo-fluid model

3. Development of a first principal vapor compression refrigeration model
4. Development of a phase change TES model
5. Integration of thermo-fluid, vapor compression, and TES models
6. Performance characterization of a baseline display case in a laboratory setting
7. Calibration of the thermo-fluid model with baseline experimentation data
8. Development of a computational fluid dynamics (CFD) model
9. Comparison of performance results of the calibrated thermo-fluid model with the CFD model
10. Development and conduction of bench-scale experimentation for the hybrid cooling system
11. Design and fabrication of TES module
12. Design and fabrication of the hybrid cooling system
13. Integration of TES module and advanced controls in the hybrid system
14. Performance characterization of the proof-of-concept hybrid display case in a laboratory setting

While the above steps are critical to the success of this project, this paper primarily focuses on the most foundational challenge associated with this innovation, which is the feasibility of product temperature maintenance via the hybrid cooling system.

Integrated Research Approach

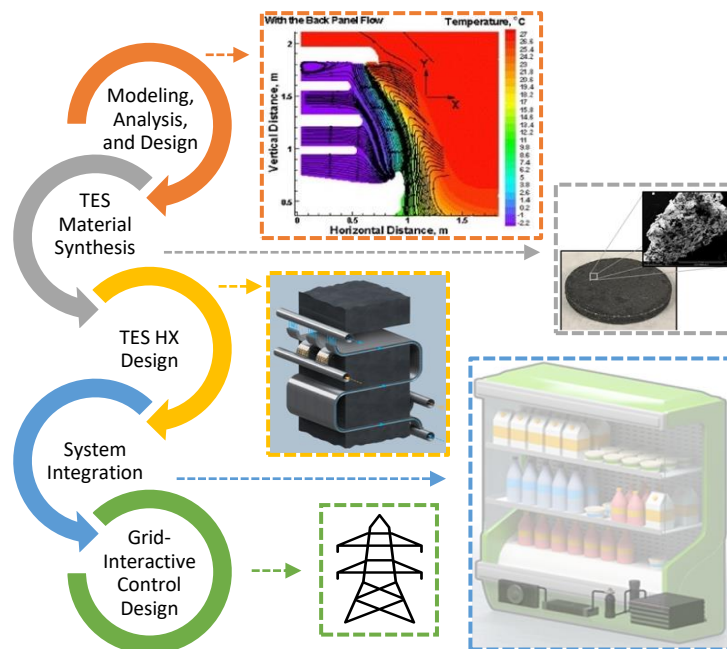


Figure 4. Integrated research approach to achieve the project goal.

Thermo-Fluid Modeling

Two independent modeling approaches and platforms were leveraged to characterize the baseline and hybrid systems. The first approach leveraged a two-dimensional thermal resistive

network model using Engineering Equation Solver (EES) and the second independent approach leveraged 3D CFD modeling. The overall approach used to formulate, validate, and optimize the baseline and proposed hybrid system performance is summarized in Figure 5.

The thermal resistive model is less computationally intensive compared to CFD and hence allows for more computationally efficient means for system parametric assessments and optimization. Nonetheless, the resistive network model considers conduction, convection, and radiation heat transfer modes and predicts the product core and surface temperatures, air psychometrics, and surface temperatures throughout the refrigerated display case. A summary of the modeling steps and validation strategy is bulletized in Figure 5.

The models reflect the geometry of an actual OVDC. Figure 6 shows a schematic of the resistive network heat transfer model formulation that was used for both the baseline and proposed hybrid system. The schematic on the left side of Figure 6 demonstrates the fluid flow in the display case in addition to the modeled convection and conduction heat transfer resistances throughout the case. The schematic on the right side of Figure 6 outlines the radiation resistance network and the associated radiative interactions between the display case, products, and surroundings. The resistive network heat transfer formulation depicted by Figure 6 is articulated as a system of coupled nonlinear equations. This system of equations is solved simultaneously and iteratively using the EES simulation engine.

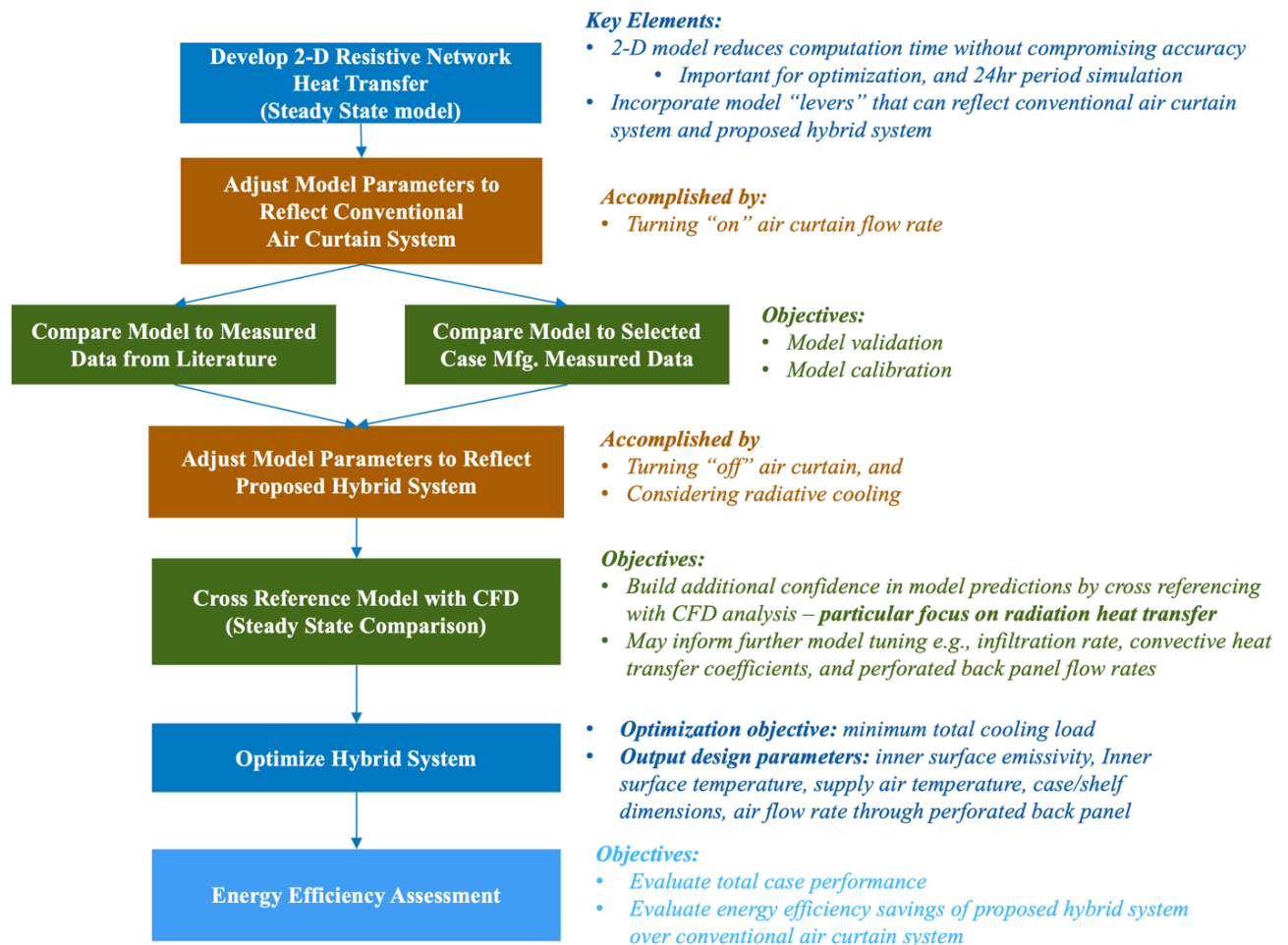


Figure 5. Modeling development and model validation workflow

Through the model, the chilled air exits the evaporator at the bottom of the fixture and travels up through the back panel of the display case. The perforated back panel allows a portion of the back panel air, dictated by some fraction of total flow rate ($\gamma[i]\dot{m}_{RAG}$), to traverse horizontally through the shelves and aid in cooling the products. The traversed air from the perforated back panel eventually rejoins the air curtain stream on the front side of the case and travels downward towards the return air grille (RAG). As the chilled air travels upward through the back panel, it exchanges heat with the rear products and the back wall of the case through an equivalent heat transfer coefficient that considers forced convection on the interior of the case, conduction through the envelope assembly, and natural convection on the exterior of the case. As the air traverses horizontally through the shelf, it exchanges heat with the products and upper shelf surface. A portion of the air traveling downward from the discharge air grille (DAG) exchanges heat with the upper shelf surface prior to mixing with infiltrated air from the surrounding space, exchanging heat with front product through forced convection. Front and back products are touching and transfer heat through conduction.

The resistive network model allows for the thermal interaction of the interior surfaces of the display case, the surroundings, and the products through various modes of heat transfer. The top surface of each product reacts with the shelf surface above, in addition to the surroundings, while considering resistances associated with radiation view factors and surface emissivities. Moreover, the front surfaces of the front products are also exposed to radiation heat transfer from the surroundings.

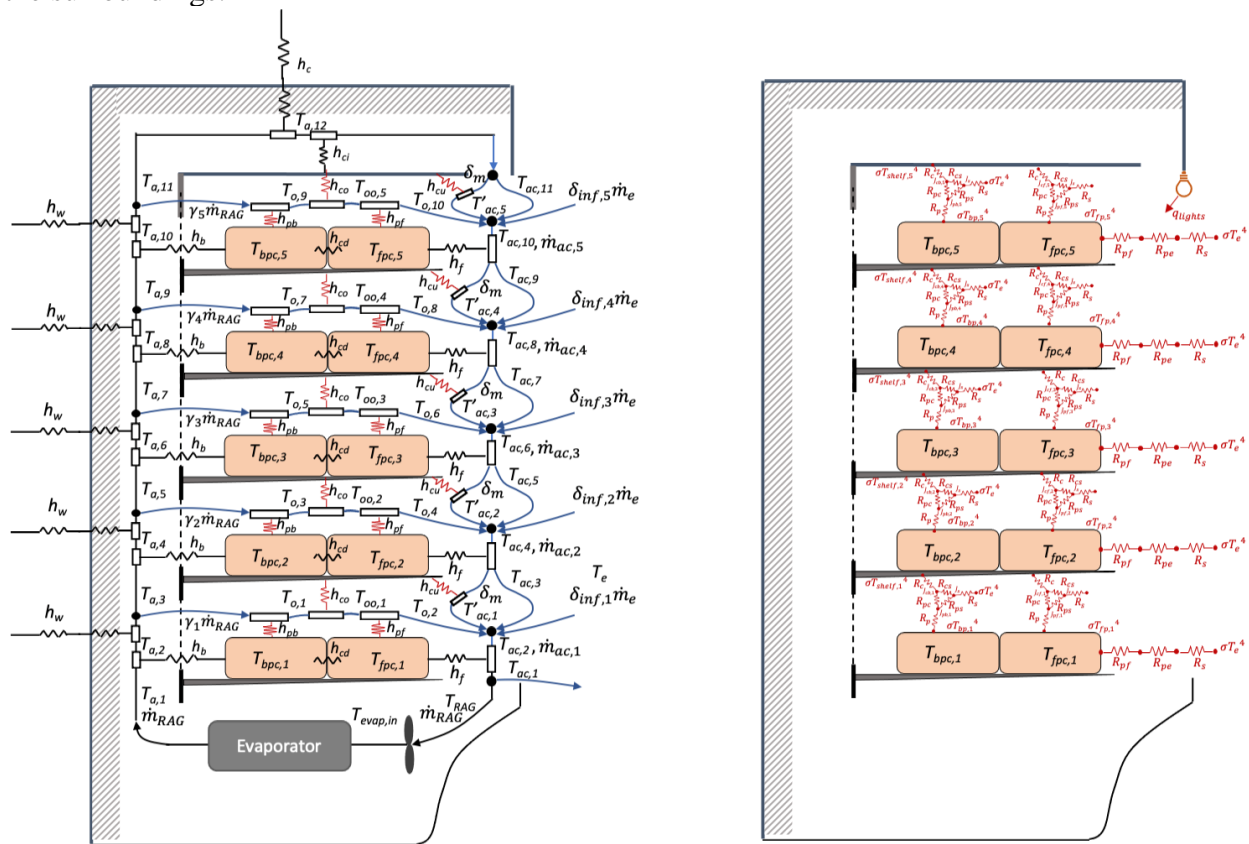


Figure 6. Resistive network model formulation of an open-vertical refrigerated display case cabinet that considers conduction, convection, and radiation heat transfer modes between the case, products, and surroundings. The schematics demonstrate the number of heat transfer resistors used in the model and their interactions.

Heat transfer coefficients, fractional mass flow rates, infiltration rate distribution per shelf, and other variables of uncertainty in the model were calibrated to measured baseline experimental data. A multivariable genetic optimization workflow was used to tune the model's variables of uncertainty. The optimization objective was minimization of mean absolute error between measured and model-predicted air and product temperatures.

CFD Modeling

The CFD modeling served as a separate analysis platform to compare the performance findings with the thermo-fluid resistive network model. Furthermore, a parametric CFD analysis helped establish the geometric features of the hybrid OVDC. Several parameters were studied during the investigation of the hybrid model. For each parameter, multiple values or configurations were computationally analyzed. These parameters include:

- Variations to return flow passage, as an alternative to the conventional RAG location
- RAG (total) flow rates needed to successfully maintain product temperatures
- Back panel flow distribution
- Solid vs. highly perforated shelves

Figure 7 is an early 3D CFD modeling result of the baseline system, depicting the temperature distribution of two perpendicular cross sections of the case.

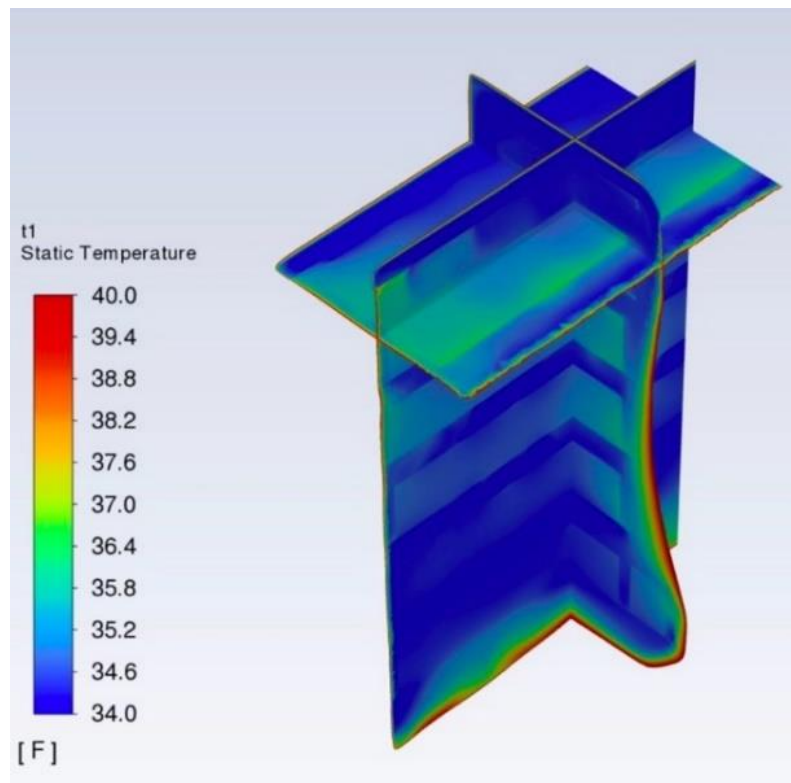


Figure 7. 3D CFD modeling result of the baseline system depicting the temperature distribution of three perpendicular cross sections of the case.

Baseline Experimentation

The purpose of this task was to perform laboratory characterization of a typical self-contained OVDC to calibrate the thermo-fluid model for achieving high confidence in model predictions. The performance of an eight-foot-long, five-deck, self-contained OVDC retrofitted with a water-cooled condenser was evaluated in a controlled-environment thermal chamber. The baseline fixture has four stacks of two shelves that are each 48” wide and 22” deep. The bottom deck is 96.25” wide and 30.5” deep. Refrigerated air exits the evaporator located at the bottom compartment and travels through a rear perforated panel to an upper DAG shown in Figure 8.

Critical temperature measurements included air (across evaporator, case interior, discharge and return grilles, and environmental control chamber), product simulators (placed throughout the case at locations based on ASHRAE Standard 72 [ASHRAE 2018]), refrigerant lines, and water lines (to the case condenser). Air temperature locations are shown in Figure 8— at each location, temperature is averaged from three probes aligned with each evaporator fan. Power consumption was measured for the total case and for the compressor, evaporator fans, lighting, and controller. Condenser coolant flow rate and pressure were measured to calculate pump hydraulic power use, and cumulative mass of condensate was measured to evaluate latent load.

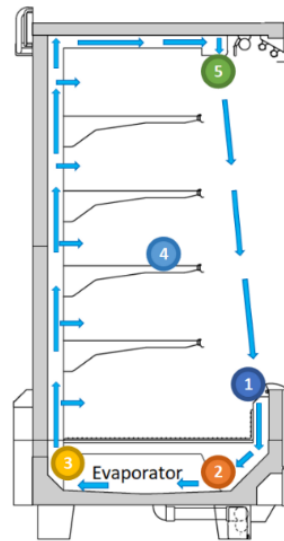


Figure 8. Baseline case convective loop and air measurement locations: (1) return air grille, (2, 3) evaporator inlet, outlet, (4) interior centroid, (5) DAG.

Experimental data were collected for a 24-hour operational period based on ASHRAE 72 and AHRI 1200 standards (AHRI 2013, ASHRAE 2018). These standards were used to maintain consistent conditions. This included the instrumentation and measurement methods, the chamber environmental conditions, and positioning of the case and product loading. Water bottles acted as filler material to simulate product thermal mass. Water inlet temperatures to the condenser were controlled to 80°F. Some 119 channels of data were monitored at a sampling rate of 1Hz. Evaluations were conducted repeatedly until approximately equivalent results were obtained between at least two 24-hour tests. A list of instruments and their corresponding accuracies for each measurement are presented in Table 1.

Table 1. List of measurement sensors and accuracy

Measurement	Brand/model	Type	Accuracy
Product simulator, air, and water immersion temperatures	Omega/TMQSS-062U-6	1/16" Type-T thermocouple probes	$\pm 0.5^{\circ}\text{C}$ ($\pm 0.9^{\circ}\text{F}$)
Chamber dew-point temperature	EdgeTech/DewTrak II DPS3	Chilled-mirror dew-point hygrometer	$\pm 0.22^{\circ}\text{C}$ ($\pm 0.4^{\circ}\text{F}$)
Refrigerant piping (and radiant panels in the hybrid cooling) surface temperatures	Omega/SA1-T-SRTC	Type-T surface temperature thermocouple	$\pm 0.5^{\circ}\text{C}$ ($\pm 0.9^{\circ}\text{F}$)
Refrigerant pressure	Omega/PX309-1KG5V	0–1,000 PSIG multimedia pressure transducer	$\pm 0.25\%$
Condensate mass	SellEton/SL7510	500-lb capacity floor scale	± 0.05 lbs
Air velocity in chamber	Kestrel 2000/312153	Wind vane anemometer	$\pm 3.00\%$
Coolant flow rate	EmersonMicromotion/CMF050M322N2 meter, 2700R12B transmitter	Coriolis flow meter	$\pm 0.05\%$
Coolant pressure	Ashcroft/G2 UPC and Omega/PX309-050GI	0–50 PSIG liquid pressure transducer	$\pm 0.50\%$ and $\pm 0.25\%$
Case total and component power	Continental Control Systems/WMC-3Y-208-MB, Accu-CT ACTL-0750	Wattnode power meter, current transformers	$\pm 0.5\%$

The modified case implementing the hybrid cooling technology will be evaluated based on its ability to maintain product temperatures within ASHRAE 72/AHRI 1200/FDA standard requirements (mean of all products never deviates outside of the 36°–40°F range over 24 hours) (ASHRAE 2018, AHRI 2013, FDA 2017). The baseline case was able to maintain steady product temperature control over 24 hours based on the standard.

Hybrid System – Bench-Scale Experimentation

For the bench-scale experimentation, custom-fit radiant panels, variable-speed evaporator fan motors/controller and a back panel with modified perforations were installed in the baseline OVDC to meet the requirements for hybrid cooling. Price Industries developed four custom panels—one mounted to the floor of the bottom deck of the case (over the evaporator), two on the left and right wall around the shelves, and one on the canopy of the case. The canopy radiant panel replaced the DAG of the baseline, and an enclosed canopy vent that directed air toward that grille from the perforated rear panel. Each radiant panel contains a copper coil seated in a

conductive trough to transfer heat from the low-emissivity panel surface. Unlike the other radiant panels, the canopy radiant panel was perforated to direct air through and downward toward the product, and so adds convective cooling through the top of the case specified in the model. Not all evaporator air is directed through the canopy panel, and some is discharged at the top edge of the rear perforated panel and leading edge of the canopy radiant perforated panel. Therefore, the case's discharge air control thermistor was relocated through the center of the rear perforated panel. Computer-aided design (CAD) drawings of the custom panels and a close-up of the copper coil and trough design are depicted in Figure 9. Images of the radiant panels mounted to the interior of the empty baseline OVDC are shown in Figure 10.

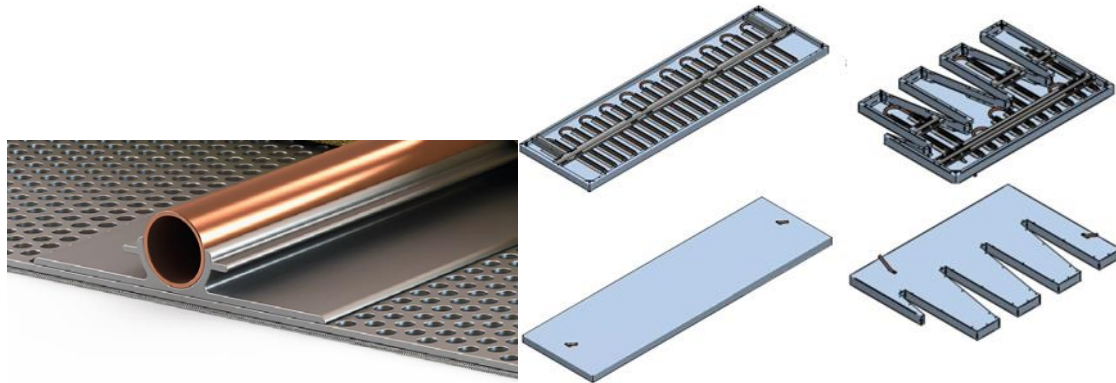


Figure 9. CAD models of the Price Industries (left) conductive coil and trough design over a perforated panel surface and (right) full panel designs used on the bench-scale hybrid case.



Figure 10. Images of the radiant panels (white surfaces) mounted to the baseline OVDC.

To remove radiative heat to the panels, a chiller supplied the panels' coils with coolant at controlled temperature and flow. Modeled conditions called for radiant panel surface temperatures of zero degrees. Because the coolant loop was external to both the case and environmental chamber, thermal losses between the chiller and panels required a low-temperature chiller with silicone coolant capable of reaching -76°F outlet temperature. The

chiller loop was constructed for parallel flow through each panel such that mean surface temperature of each radiant panel could be balanced as close to 32°F as possible by adjusting flow between panels. A simplified piping and instrumentation diagram (P&ID) and image of the setup radiant panel coolant loop are shown in Figure 11.

The baseline case’s evaporator fan motors were replaced with Epec-brand ECY-03 model motors capable of variable-speed control with equivalent performance and electrical specifications, and near-equivalent input/output power at full speed. Fan speed was controlled by varying the input voltage. To modify the orientation of perforations through the rear panel (non-radiant for directing convective cooling air) according to the design determined from CFD modeling, a replacement back panel was modified from the case manufacturer.

To evaluate the hybrid bench-scale case, all instrumentation used in the baseline evaluation was included in the bench scale. Discharge air measurements were relocated to the space between the top edge and leading edge of the rear perforated panel and canopy radiant panel as the DAG was removed. Additional instruments were also included to evaluate the performance of the radiant component to the hybrid cooling mechanism as shown in the P&ID in Figure 11. These included the same models of Coriolis flowmeter (“CF”), insertion probe thermocouples (“IPT”), and surface thermocouples (“ST”) used in the baseline evaluation listed in Table 1, except for the turbine flowmeters or rheometers (“R” in Figure) used for the individual panel flows. Those are Omega brand, BV2000 model flowmeters with ±3% accuracy. The thermal loads of the system and individual panels are calculated using the temperature and flow entering and leaving the chiller and radiant panels.

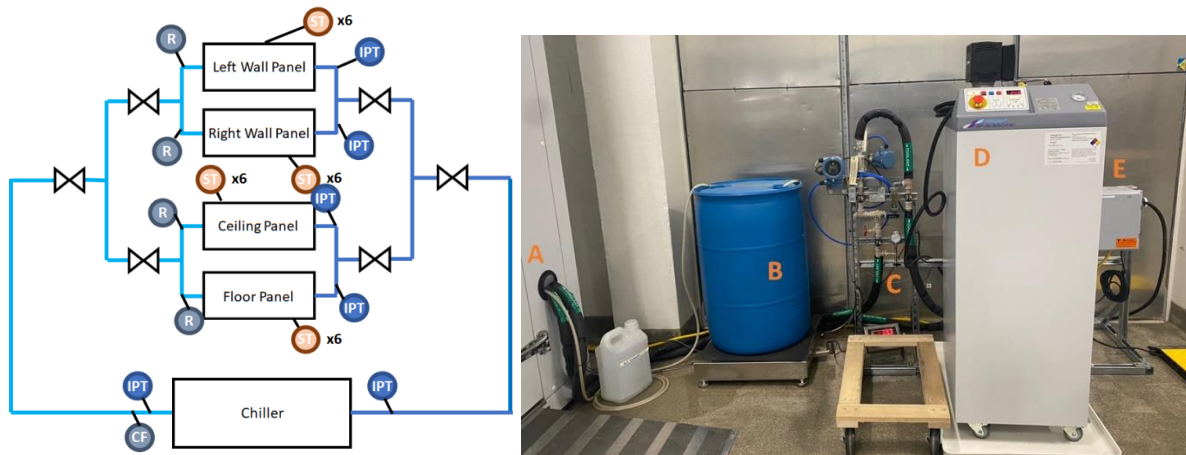


Figure 11. P&ID and image of chiller coolant line configuration to the radiant panels. A: port into/out of chamber; B: condensate drum and scale; C: flowmeters, pressure gauges, and thermocouples; D: chiller; and E: control box for the chiller, valves, and flood switches to detect leaks.

Surface thermocouples were used to control chiller conditions to meet modeled panel conditions. Six thermocouples were evenly spaced on each panel at the corners and center-front and rear locations aligned with the center of the furthest bend in each underlying copper coil. The upgraded hybrid bench-scale case was oriented in the environmental chamber in the same manner as the baseline case according to ASHRAE 72 standard requirements. Images of the case inside the chamber are shown in Figure 12.

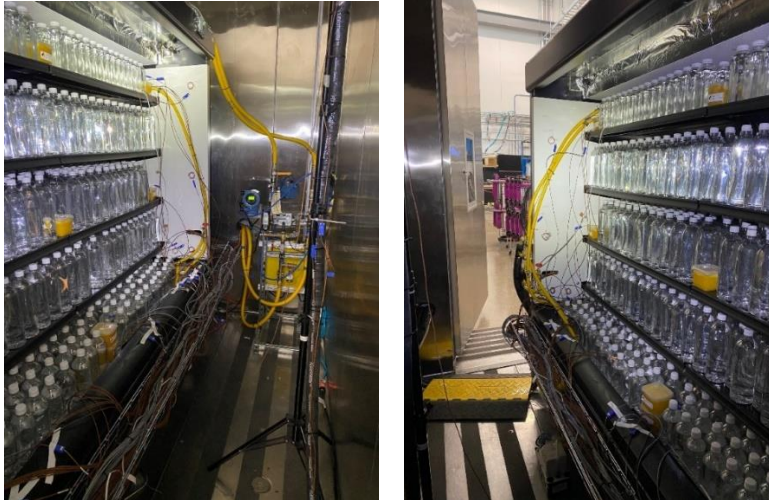


Figure 12. Image of the case setup inside the environmental chamber from (left image): front, (right image): rear.

Results

Figure 13 demonstrates the CFD and EES modeling results associated with the baseline system. Moreover, Figure 13 shows the experimental core product, RAG, and DAG measured temperatures for comparison. Both CFD and EES baseline models are closely aligned with measured data, demonstrating a mean absolute error between modeled and measured product and air temperatures of 0.25°F . Figure 13 also summarizes the breakdown of the EES model-predicted cooling load into its associated constituents.

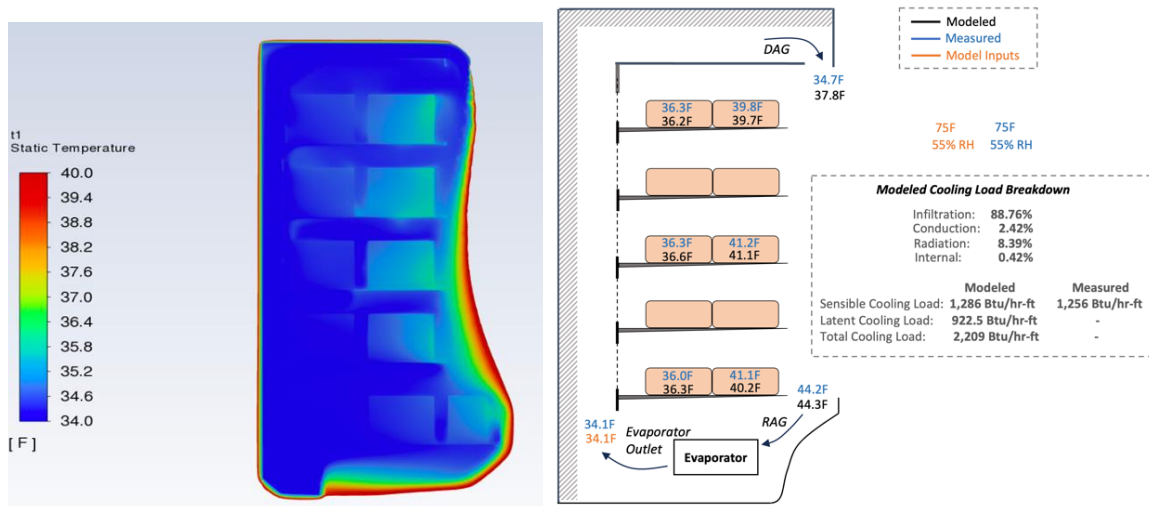


Figure 13. CFD baseline model results (left) and resistive network baseline model results (right).

The CFD model was particularly useful at informing the required back panel air flow and associated perforation per shelf location that would enable minimal and optimally distributed air flow (convective cooling) while maintaining product temperatures. The results showing the optimal flow distribution through the perforated back panel and its associated relative locations per shelf are shown in Figure 14.

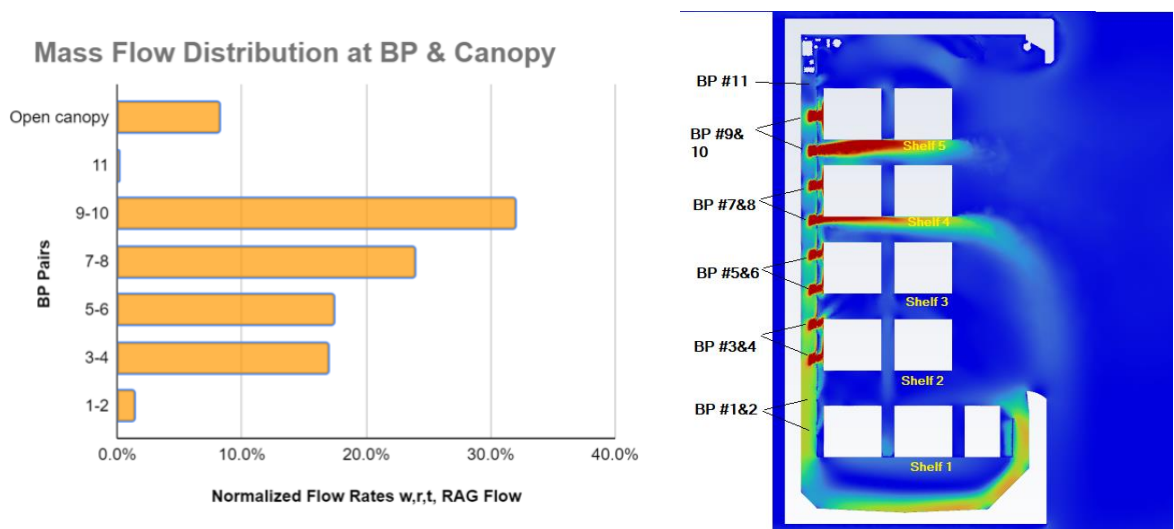


Figure 14. Normalized back panel (BP) flow rate vs. row numbers (left), and back panel jet flow positions relative to the shelves (right).

A comparison of the average core product temperatures between EES and CFD is summarized in Table 2. EES and CFD predictions are in close agreement and within 0.2°F temperature difference.

Table 2. Average product temperatures from EES, CFD, and experimental measurements

	EES (<i>model approach 1</i>)	CFD (<i>model approach 2</i>)
Baseline system	38.4°F	38.2°F
Hybrid system (<i>bench-scale</i>)	39.2°F	39.1°F

Initial bench-scale experimentation included evaluating the case product temperatures with only the radiant cooling to understand its isolated effect. Under steady-state conditions, with a mean radiant panel surface temperature of 31.8°F and ASHRAE environmental conditions inside the control chamber, the average product temperature was held to 45.5°F initially and 47.0°F (where the upper regulatory limit is 40.0°F) after balancing flow rates to achieve mean panel surface temperatures as close as possible to 32°F. Radiant cooling was sufficient for cooling products at the rear of the case. However, product at the front of the case exposed to ambient chamber air was only able to cool by at least 7 degrees and bottom-shelf products were overcooled and frozen through conduction.

Both the EES and CFD models required ancillary cooling via forced convection at 50% of the baseline flow rate. Phase 2 experiments were therefore then conducted at incremental fan speeds. The baseline airflow was generated at a constant evaporator fan speed of 1600 RPM. Therefore, to optimize the air flow rate, performance of the bench-scale hybrid was evaluated between a minimum 500 RPM and maximum 1600 RPM. The case was able to maintain product temperatures according to standard requirements only at fan speeds above 800 RPM. The mean

temperature approached the upper regulatory limit with increasing speed and surpassed the limit between 800 and 900 RPM. It was realized, however, that the duct pressure drop is now much higher in the modified bench-scale hybrid case than the baseline due to the replacement of the canopy and DAG with the perforated canopy panel. Therefore, 800 RPM is generating a lower airflow rate than at 50% modeled.

At the lower fan speeds where the case was unable to meet the ASHRAE limit, the dominant cooling mechanism was clearly not from forced convection through the evaporator, but rather through combined radiant cooling and convection over the radiant panel. This is evident from the low difference in temperatures across both cases' heat exchangers which are sustained through compressor cycles ($\Delta T_{\text{evaporator}}$ ranged between only 1.46°F and 3.02°F), and which prevented the compressor from cycling more than briefly. The low differential caused by extremely cold evaporator inlet temperatures indicated that at low evaporator fan speeds, conduction through the bottom of the floor panel dominates and overcools the evaporator panel space.

At these lower evaporator fan speeds, average product temperature was affected by high temperatures on the front and middle of the case and low temperatures across the bottom shelf, the same as observed with the radiant-only experiments. The product on the top-front of the case will only become slightly cooler than the ambient dry bulb temperature with too little convection over it. The air temperatures throughout the case, which would increase significantly as the air traveled up the rear perforated panel and then lower at the canopy panel, also indicated that not enough convection is being provided by the evaporator fans.

In addition to meeting mean product temperatures within ASHRAE/AHRI/NSF requirements, evaporator fan speeds over 800 RPM allowed the case to maintain product control within a tighter range of minimum and maximum temperatures, although the range at 1000 RPM was not quite as tight as the baseline. The results of these experiments are shown in Table 2.

Table 2. Summary of results from hybrid radiant and convective cooling experiments

Test (evaporator fan speed)	Mean panel surface temperature	Mean product temperature	Maximum product temperature	Minimum product temperature	Condensate weight
500 RPM (min)	29.77 ± 9.68°F	42.12°F	62.24°F	18.30°F	2.3 lbs
700 RPM	25.05 ± 9.45°F	40.57°F	61.12°F	17.38°F	1.8 lbs
800 RPM	25.75 ± 10.58°F	40.19°F	61.14°F	17.11°F	2.1 lbs
1000 RPM	30.42 ± 8.23°F	38.84°F	49.30°F	25.05°F	34 lbs
1200 RPM	28.98 ± 8.35°F	37.54°F	45.32°F	25.11°F	33 lbs
1600 RPM (max)	29.41 ± 7.56°F	37.96°F	45.54°F	27.28°F	93 lbs

At higher evaporator fan speeds of 1000–1600 RPM, the warmest and coldest product temperatures began approaching ASHRAE/AHRI/NSF-7 limits. This indicated that additional forced air convection was needed through the canopy panel and over the bottom shelf. The observed air temperatures also imply that forced convection through the evaporator adequately augmented the hybrid cooling capacity.

Conclusions

Preliminary findings indicate that the proposed hybrid design, comprised of radiant cooling coupled with moderate forced air convection through the back panel, can achieve an acceptable mean product temperature. The hybrid design eliminated the inefficient air curtain mechanism and delivered mean product temperatures between 36°F and 39°F with radiant panels maintained within the 21°F–31°F range, and with evaporator air flows starting at 50% of the baseline.

Additionally, a strong confidence in the first principal thermo-fluid predictions was established through the convergence with CFD and bench-scale experimental results. The validated thermo-fluid model will be further leveraged to identify strategies for minimizing the cooling load of the case.

The next steps of the project will include developing design specifications for fabrication of a hybrid proof-of-concept fixture. The hybrid proof-of-concept will include TES and advanced controls integration. The project will then ascertain the energy efficiency benefits of the hybrid proof-of-concept, and assess the impacts of load flexibility strategies by leveraging the TES system in a laboratory setting.

References

AHRI (Air-Conditioning, Heating, and Refrigeration Institute). 2013. Standard for Performance Rating of Commercial Refrigerated Display Merchandisers and Storage Cabinets. ANSI/AHRI.

ASHRAE. 2018. Method of Testing Open and Closed Commercial Refrigerators and Freezers. ANSI/ASHRAE.

EIA (U.S. Energy Information Administration). 2018. Forms EIA-871A, C, D, E, and F of the 2018 Commercial Buildings Energy Consumption Survey.

Faramarzi, R., B. Coburn, and R. Sarhadian. 2002. “Performance and energy impact of installing glass doors on an open vertical deli/dairy display case.” *ASHRAE Transactions* 108:673-679.

FDA (U.S. Food and Drug Administration). 2017. Food Code 2017, in U.S. Public Health Service. U.S. Department of Health and Human Services.

Hirsch, A., J. Clark, M. Deru, and K. Trenbath. 2015. “Pilot Testing of Commercial Refrigeration-Based Demand Response.” Golden, CO: National Renewable Energy Laboratory. <https://www.nrel.gov/docs/fy16osti/65009.pdf>

Jackson, J. 2020. “Evaluating Supermarket Energy Management Strategies, Emerson Commercial & Residential Solutions.” <https://emersonclimateconversations.com/2020/01/14/evaluating-supermarket-energy-management-strategies/>